

# Controlled radical polymerization of methyl methacrylate mediated by copper complexes with iminopyrrolyl ligands

Henrique T. Matos<sup>1</sup>, Tiago F. C. Cruz<sup>1</sup>, Rui B. Dias<sup>2</sup>

<sup>1</sup> Departamento de Engenharia Química, Instituto Superior Técnico, Universidade de Lisboa, Av. Rovisco Pais, nº 1, 1049-001 Lisboa, Portugal

<sup>2</sup> SGL Composites, S.A, Rua 53 Parque Industrial da Quimigal, 2830-138 Barreiro, Portugal;

*The role of copper(I) complexes containing 2-iminopyrrolyl chelating ligands and phosphine ligands together with a bromo-alkyl ester in the formation of suitable initiator systems for methyl methacrylate controlled radical polymerization was studied. Various 2-iminopyrrolyl chelating ligands were tested, the ones showing less steric hindrance around the metal center of the complex or higher electronic donating capabilities yielding better results in terms of activity and controllability of the polymerization. Moreover, by exchanging the phosphine ligand from triphenylphosphine to trimethylphosphine it was possible to lower the molecular weight distribution of the polymer and increase the activity even further. In fact, the initiator system composed of [Cu{κ<sup>2</sup>N,N'-NC<sub>4</sub>H<sub>3</sub>-2-C(H)=NCH<sub>3</sub>}(PMe<sub>3</sub>)<sub>2</sub>] (10)/tert-butyl-α-bromoisobutyrate (11) at 90 °C and molar ratio of monomer:initiator:complex 500:1:1 led to a reasonable control of the molecular weight distribution and dispersity, closer to a typical Atom Transfer Radical Polymerization (ATRP) mechanism. The other complexes yielded polymers with higher dispersities and molecular weights than expected. Cyclic voltammetry studies of the copper(I) complexes used pointed to an effect of the steric and electronic environment around the metal center of the complex on the oxidation reaction to copper(II). An almost linear trend was observed, in which increasing polymerization activities were correlated with decreasing peak potentials relative to the oxidation of the metal center to copper(II).*

**Keywords:** controlled/living radical polymerization, MMA, ATRP, copper(I) complexes

## Introduction

The mechanism for living anionic polymerization was discovered by Szwarc *et al.*,<sup>1</sup> in 1956, triggering the eventual development of controlled radical polymerization (CRP). In this type of polymerization, chain-breaking reactions, such as chain transfer or termination are minimized (or eliminated), by establishing an equilibrium between propagating radicals and a dormant species. Deactivation of the dormant species leads to the protection of the propagating chain. This deactivation must be reversible, thus turning the propagating chain into a living status and susceptible to the addition of further monomer units. Chain growth is achieved by successive and rapid activation/deactivation steps of the dormant species. In a controlled polymerization, the monomer addition should follow a first order kinetics, molecular weight should be proportional to

monomer conversion, dispersity should follow a Poisson type distribution and decrease with monomer conversion and every chain should be end-functionalized. In terms of the mechanism, the equilibrium between propagating radicals and dormant species, can be achieved with three different approaches (Fig. 1).<sup>2</sup> In controlled radical polymerization by SFRP (stable Free Radical Polymerization), a radical species, X<sup>\*</sup>, is involved in the activation/deactivation equilibrium of the propagating polymer chain. This species is usually a nitroxide or an organometallic/coordination compound (Fig. 1a). In ATRP (Atom Transfer Radical Polymerization), a species Y, an organometallic/coordination compound, establishes an equilibrium with a halogen atom, X, by way of a redox reaction. The halogen is thus responsible for the quick protection/deprotection of the polymer chain

(Fig. 1b). On the other hand, in degenerative transfer radical polymerization (DT), the initiation mechanism is conventional, or analogous to free radical initiation, and the control is achieved by means of a transfer agent, X (Fig. 1c).

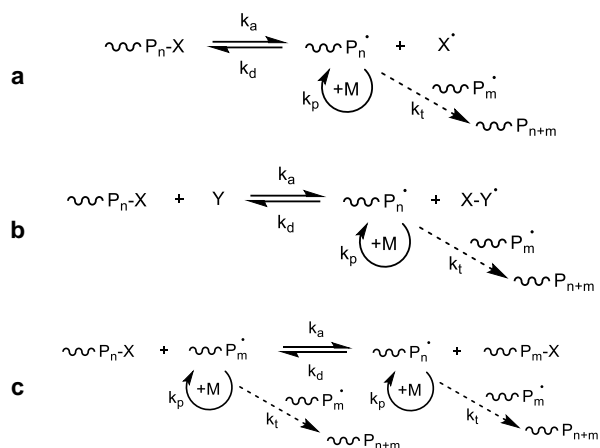


**Fig. 1** Simplified controlled radical polymerization mechanisms: (a) SFRP; (b) ATRP; (c) DT.

Copper was one of the first transition metals whose complexes were successfully used in controlled radical polymerization and is still one of the most studied. It proved to be very versatile, working with a wide array of solvents and conditions, and due to its widespread use, many initiators and ligands are commercially available. Besides this, it has been applied to the controlled polymerization of an extensive list of monomer families, such as acrylates, methacrylates, acrylamides, methacrylamides and styrene derivatives.<sup>3</sup>

Apart from the normal ATRP mechanism, new advances have been made to lower the copper concentration required, to increase the oxygen tolerance and to allow the reaction to be performed in different solvents, especially in water.<sup>3</sup> Examples of these derivations are ARGET ATRP (Activators Regenerated by Electron Exchange) systems, which use reducing agents to regenerate the activators and therefore can lower the amount of copper used to just a few ppm.<sup>4</sup> Alternatively, eATRP technology applies an electric current to force the regeneration of the activators.<sup>5</sup> With this method

polymerization rates can be tuned by changing the applied current, potential, and total passed charge.<sup>6</sup>

In this work, we studied the controlled radical polymerization of methyl methacrylate (MMA) using as a reaction system a 500:1:1 or 100:1:1 ratio of MMA to radical initiator (*tert*-Butyl  $\alpha$ -bromoisobutyrate) to copper(I) complex. All studied complexes **1-10** are stabilized by a phosphine ligand (triphenylphosphine, PPh<sub>3</sub>, or trimethylphosphine, PMe<sub>3</sub>) and a 2-iminopyrrolyl bidentate chelating ligand. Both the type of chelating and supporting ligands were varied, to study the effect of the electronic and steric environment around the metal center of the complex on the kinetics and controllability of the polymerization reactions.

A general formula of the copper(I) complexes **1-10** used in this work is shown in Fig. 2. These complexes, stabilized by phosphines, are tetrahedral 18-electron species with the copper centers in the oxidation state +1, which can be efficient in one-electron transfer processes by oxidation to the +2 state, dissociating of one of the phosphines, to a 17-electron species. The initiator, *tert*-butyl  $\alpha$ -bromoisobutyrate (**11**, Fig. 3), was selected from typical commercial initiators used in ATRP processes, allowing the formation of very stable tertiary radicals. The list of the substituents and ligands used in each copper(I) complex are presented in Table 1.

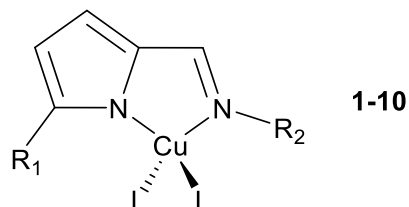


**Fig. 2** Copper(I) complexes tested in the controlled radical polymerization of MMA throughout this study (R<sub>1</sub> and R<sub>2</sub> substituents and L ligands are summarized in Table 1).

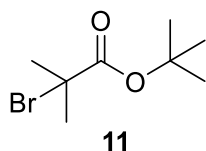


**Fig. 3** Radical initiator used in the polymerization tests.

**Table 1** List of copper(I) complexes tested in this study.

Complex	R <sub>1</sub>	R <sub>2</sub>	L
1	H	phenyl	PPh <sub>3</sub>
2	H	2,6-diisopropylphenyl	PPh <sub>3</sub>
3	H	4-dimethylaminophenyl	PPh <sub>3</sub>
4	H	4-ferrocenylphenyl	PPh <sub>3</sub>
5	1-Adamantyl	1-Adamantyl	PPh <sub>3</sub>
6	phenyl	phenyl	PPh <sub>3</sub>
7	H	2,6-dimethylphenyl	PPh <sub>3</sub>
8	H	methyl	PPh <sub>3</sub>
9	2,6-dimethylphenyl	2,6-diisopropylphenyl	PPh <sub>3</sub>
10	H	methyl	PMe <sub>3</sub>

## Results and Discussion

**Synthesis and characterization of the Cu(I) complexes:** The synthesis of the copper(I) complexes started by the preparation of the respective sodium salt of the 2-iminopyrrolyl ligand by *in situ* deprotonation of the ligand precursor with NaH in THF. The 2-iminopyrrole ligand precursors were previously synthesized according to the procedure available in the literature.<sup>7–11</sup> The copper(I) starting material, [Cu(NCMe)<sub>4</sub>]BF<sub>4</sub>, previously synthesized following the procedure detailed in the literature,<sup>12</sup> was reacted with 2 equivalents of the respective phosphine. After 30 minutes, the solution containing the sodium salt of the ligand was filtered dropwise into the Schlenk containing the copper(I) starting material mixture, at -20 °C – Fig. 4. The copper complexes were obtained by evaporation of the cloudy solution, followed by *n*-hexane, diethyl ether, or toluene extractions, in good yields.

Similarly, the synthesis of a copper(I) complex stabilized with tricyclohexylphosphine (PCy<sub>3</sub>), a novel compound, was attempted, unsuccessfully. This phosphine has a larger Tolman cone angle than PPh<sub>3</sub> and PMe<sub>3</sub>,<sup>13</sup> which makes it difficult for both phosphines to coordinate to the copper atom. The novel coordination complexes synthesized during this study (**7**, **8** and **10**) were characterized by <sup>1</sup>H, <sup>13</sup>C(APT) and <sup>31</sup>P{<sup>1</sup>H} NMR, by <sup>1</sup>H-<sup>1</sup>H (COSY), <sup>1</sup>H-<sup>13</sup>C (HSQC), elemental analysis and, whenever possible, by X-ray diffraction.

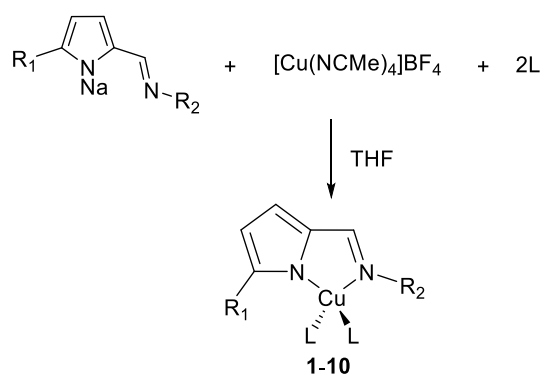


**Fig. 4** Preparation of the Cu(I) complexes **1-10** (R<sub>1</sub> and R<sub>2</sub> substituents and L ligands are summarized in Table 1).

The molecular thermal ellipsoid diagrams for complexes **8** and **10** are shown, derived from the X-ray diffraction studies are presented in Fig. 5 and Fig. 6.

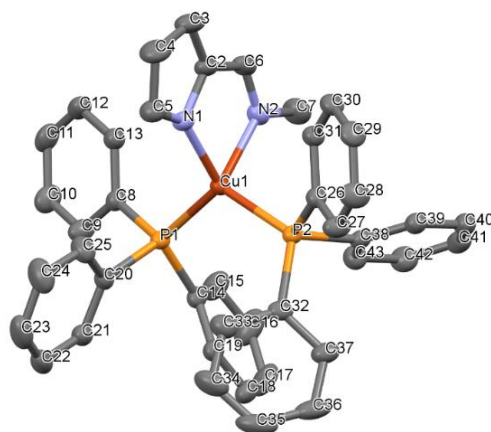


**Fig. 5** Molecular structure of complex **8**, using 50% probability ellipsoids. Hydrogen atoms are omitted for clarity.

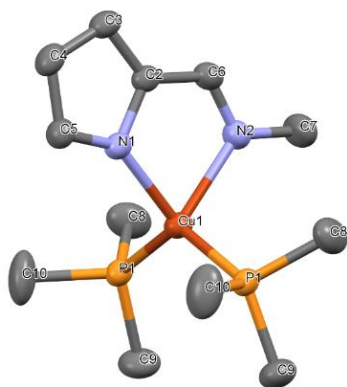


**Fig. 6** Molecular structure of complex **10**, using 50% probability ellipsoids. Hydrogen atoms are omitted for clarity.

Complexes **8** and **10** present a tetrahedral coordination geometry, with one 2-iminopyrrolyl bidentate ligand and two adjacent phosphine ligands. The Cu1-N and Cu1-P bond lengths were found to be between 2.038(2) and 2.108(2) Å and between 2.213(4) and 2.252(4) Å, respectively. These latter bonds are marginally shorter for complex **10**.

**Initial behavior of the initiator system:** According to preliminary polymerization tests, the reaction is halted by exposure to air, with a visible color change due to the oxidation of the coordination complex. The high sensitivity to air is justified by the reactivity of the free radicals generated with the molecular oxygen. Additionally, the copper(I) complexes are also sensitive to air as the metal center easily oxidates in the presence of oxygen and the nitrogen of the pyrrolyl of the chelating ligand is highly basic, being easily protonated by residual water molecules. Besides this, the presence of phosphine ligands, which present high lability, and the existence of vacant d orbitals in the phosphorus, makes them easily oxidated to triphenylphosphine oxide (O=PPh<sub>3</sub>) or trimethylphosphine oxide (O=PMe<sub>3</sub>).

With an initiator system composed of a copper(I) complex (**8**), without a radical initiator, no polymer was observed after 16 h at 90 °C. When the reaction was performed with the radical initiator, but

without the coordination complex, no polymer was observed after 2 h, and only a small amount of polymer was present after 5 h (corresponding to a conversion of about 11%). The polymer observed is formed by thermally initiated free radical polymerization. Using complex **1** a monomer conversion of 25% was achieved after 6 h at 90 °C and molar ratio of monomer:initiator:complex of 500:1:1.

### Effect of the variation of the copper(I) complex on the polymerization kinetics:

The influence of the type of copper(I) complex used on the propagation rate and polymerization control was studied. To this effect, the ligand precursor was varied, to alter the steric and electronic environment around the metal center of the complex. Furthermore, the influence of the phosphine ligand structure on the stabilization of the complex, and therefore on its activity on the polymerization was also studied. The results for the evolution of  $\ln([M]_0/[M])$  with time are presented in Fig. 7, for the polymerization of MMA at 90 °C and monomer:initiator:complex molar ratio of 500:1:1. The apparent rate constant of propagation,  $k_p'$ , for each test is summarized in Table 2, given by the slope of a linear regression for  $\ln([M]_0/[M])$  vs  $t$ .

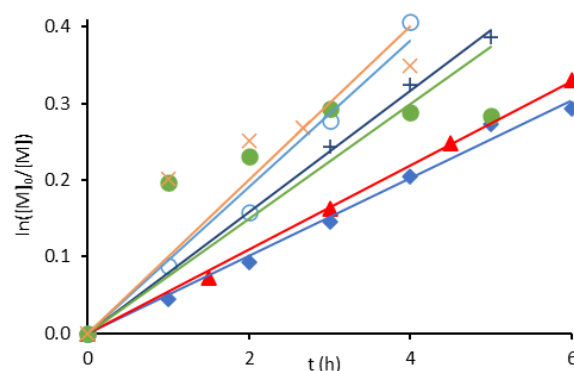


**Fig. 7** Representation of  $\ln([M]_0/[M])$  vs  $t$ , for MMA polymerizations performed at 90 °C and molar ratio  $[M]:[I]:[C]$  500:1:1, for various copper(I) complexes:  $\blacklozenge$  - **1**;  $\blacktriangle$  - **2**;  $\circ$  - **3**;  $\square$  - **7**;  $\bullet$  - **8**;  $\times$  - **10**.

**Table 2** Apparent propagation rate constants for each complex tested, in descending order.

Complex	$k_p'$ ( $\text{h}^{-1}$ )
10	$(1.00 \pm 0.06) \times 10^{-1}$
3	$(9.56 \pm 0.39) \times 10^{-2}$
7	$(7.49 \pm 0.61) \times 10^{-2}$
8	$(7.48 \pm 1.12) \times 10^{-2}$
2	$(5.47 \pm 0.06) \times 10^{-2}$
1	$(5.07 \pm 0.11) \times 10^{-2}$

The copper(I) complexes with  $R_1$  substituents were inactive in the polymerization of MMA in the tested conditions, possibly due to the excessive steric stress of these substituents. Apart from these, complex 4 was also inactive in the polymerization of MMA, possibly due to the irreversible oxidation of the 4-ferrocenylphenyl by the bromide radical.

Complex 3 showed a good activity in the polymerization. This complex is stabilized by the 4-dimethylaminophenyl  $R_2$  substituent, through an electronic donation effect. Comparing the results from complexes 1 ( $R_2$ =phenyl), 2 ( $R_2$ =2,6-diisopropylphenyl) and 7 ( $R_2$ =2,6-dimethylphenyl), there is not a clear influence of the steric hindrance by the aromatic ring at  $R_2$  on the polymerization kinetics. Other effects can also play a role, such as electronic donation. By exchanging the aromatic ring at  $R_2$  for a methyl group (8), the polymerization rate increased, possibly due to a lower steric hindrance. A further increase in activity was observed when using  $\text{PMe}_3$  as a support ligand (10), being indeed the complex with the highest value of  $k_p'$  among the ones studied. Trimethylphosphine ligands have a strong  $\sigma$ -donor character, stabilizing the metal center, and a lower Tolman cone angle, therefore lower steric hindrance.

**Molecular weight distribution analysis:** Besides evaluating if the evolution of the monomer conversion with time follows a first order kinetic equation, it is necessary to assess the controllability in terms

of the molecular weight and dispersity to conclude if the polymerization is controlled.

By varying the type of copper(I) complex used, it was observed that all samples had a molecular weight (measured by GPC/SEC) higher than what would be expected from a living radical polymerization. The polymerization using complex 2 generated PMMA samples with the highest  $M_n$ . On the other hand, complexes 7, 8 and 10 showed better results in terms of the controllability of the polymer molecular weights, with values closer to the theoretical  $M_n$  line (Fig. 8). A trend was observed between the decrease in steric hindrance around the metal center of the complex, by substituting the isopropyl groups (2) with methyl (7), and an increase in the molecular weight controllability for the MMA polymerization. The inductive effect caused by the *ortho* methyl groups on the aromatic ring (7) also likely helped to decrease the values of  $M_n$ , when comparing with complex 1 (Fig. 8).

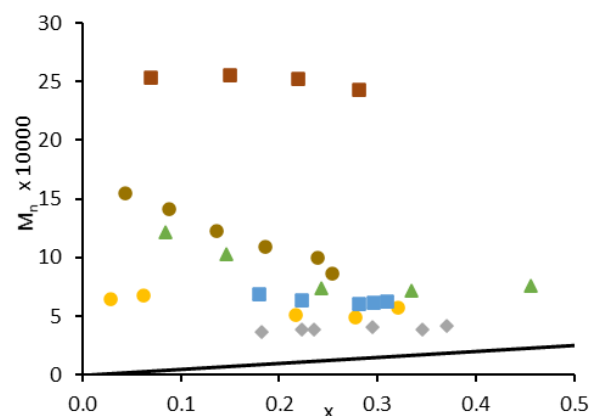


**Fig. 8** Evolution of the molecular weight distribution,  $M_n$ , with the MMA conversion, at 90 °C and molar ratio  $[\text{M}]:[\text{I}]:[\text{C}]$  500:1:1, by varying the copper(I) complex: ● - 1; ■ - 2; ▲ - 3; ○ - 7; ■ - 8; ◆ - 10; — - theoretical.

The controllability in terms of dispersity was not achieved with any of the complexes tested, with many of the samples showing  $\text{Đ} \approx 2$  for the polymerizations performed at 90 °C. The best results were obtained for the complex 10, with a dispersity varying from 1,6 to 1,8. Moreover, replacing the phosphine ligand  $\text{PPh}_3$  (8) with  $\text{PMe}_3$  (10), increased the

controllability of the system, yielding the best results from among all the complexes tested.  $\text{PMe}_3$  is a better  $\sigma$ -donor, therefore facilitating the oxidation of the copper(I) center, which leads to a more efficient coordination/discoordination equilibrium. The activation/deactivation equilibrium is, thus, shifted to the left, minimizing transfer or chain termination reactions.

**Cyclic voltammetry:** Complexes **1**, **2**, **3**, **4**, **7**, **8** and **10** were analyzed using cyclic voltammetry. In Fig. 9, the voltammograms of complexes **1**, **3** and **4** are compared, which vary in the *para* substituent of the aromatic ring in  $\text{R}_2$ . Complex **1** has two oxidation peaks corresponding to two irreversible oxidation steps. The first one appears to be the oxidation of the metal center, from copper(I) to copper(II). Complex **3** shows a multitude of peaks, the first one related to the oxidation to copper(II), which appears at a lower  $E_p$  value. Complex **4** has a reduction peak associated with the first oxidation step, corresponding to the ferrocene, because it has an  $E_{1/2}$  value of  $-0.01$  V, which is within the experimental error for the  $E_{1/2}$  of FcH. This should be due to an impurity, and thus  $E_{p2}$  corresponds to the oxidation of copper(I).

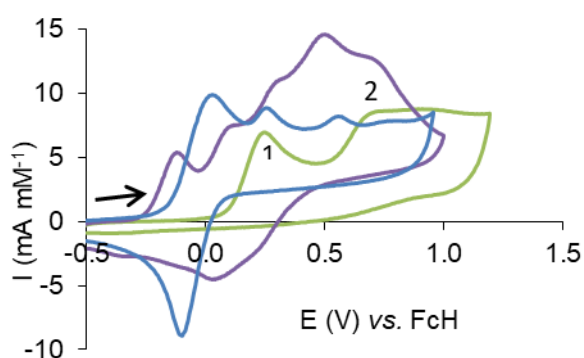


**Fig. 9** Cyclic voltammograms ( $200 \text{ mV s}^{-1}$ ) for complexes **1** (—, -H), **3** (—,  $-\text{NMe}_2$ ) and **4** (—, -Fc).

In Fig. 10, the voltammograms of complexes **1**, **2** and **7** are compared, which vary in the *ortho* substituent of the aromatic ring in  $\text{R}_2$ . The values of  $E_{p1}$  are not very different, which indicates that changes

made in the structure of the chelating ligand do not have a great influence on the ease of the oxidation of the copper(I) complex. A slight decrease in  $E_{p1}$  is observed, however, for complex **7**, probably due to the electronic donation effect caused by the methyl groups.

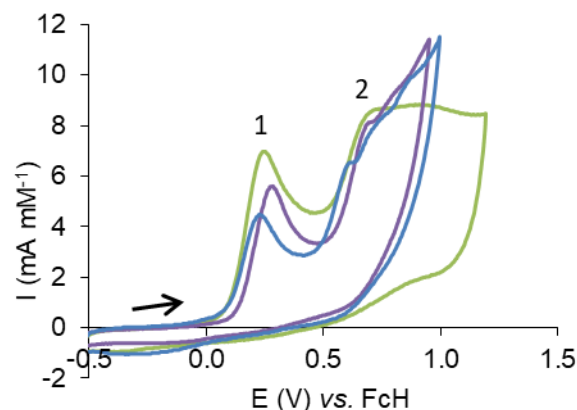


**Fig. 10** Cyclic voltammograms ( $200 \text{ mV s}^{-1}$ ) for complexes **1** (—, -H), **2** (—,  $-i\text{Pr}$ ) and **7** (—, -Me).

In Fig. 11, the voltammograms of complexes **8** and **10** are compared, which vary in the type of phosphine ligand used to stabilize the complex. As the  $E_{p1}$  for complex **10** is lower than for complex **8**, the first one oxidizes more easily, probably due to a lower steric hindrance by  $\text{PMe}_3$  and a higher  $\sigma$ -donor character when compared to  $\text{PPh}_3$ .

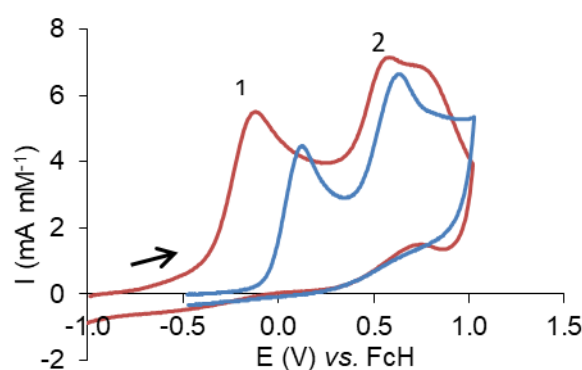


**Fig. 11** Cyclic voltammograms ( $200 \text{ mV s}^{-1}$ ) for complexes **8** (—,  $-\text{PPh}_3$ ) and **10** (—,  $-\text{PMe}_3$ ).

The results for the values of peak potentials of each complex are summarized in Table 3, in ascending order of  $E_{p1}$ .



**Table 3** Oxidation peak potentials for the copper(I) complexes studied, in ascending order of  $E_{p1}$ .

Complexo	$E_{p1}$	$E_{p2}$	$E_{p3}$	$E_{p4}$
<b>10</b>	-0.15	0.55	-	-
<b>3</b>	-0.12	0.10	0.30	0.49
<b>4</b>	0.05	0.29	0.58	-
<b>8</b>	0.12	0.62	-	-
<b>7</b>	0.23	0.63	-	-
<b>1</b>	0.29	0.78	-	-
<b>2</b>	0.32	0.75	-	-

As represented in Fig. 12, by analyzing the relationship between the  $E_{p1}$  value for each complex and the respective value of  $k_p'$ , a quasi-linear trend is observed. Therefore, the copper(I) complexes that oxidized more readily were more active in the polymerization of MMA. In fact, complex **10** has the highest value for  $k_p'$  and the lowest  $E_{p1}$  and, as was observed by the analysis of the molecular weight distributions, allowed for a better control of the molecular weight. This means that the design of the complexes used for the controlled radical polymerization should, not only be focused on the chelating ligand, but also on the respective support ligand.

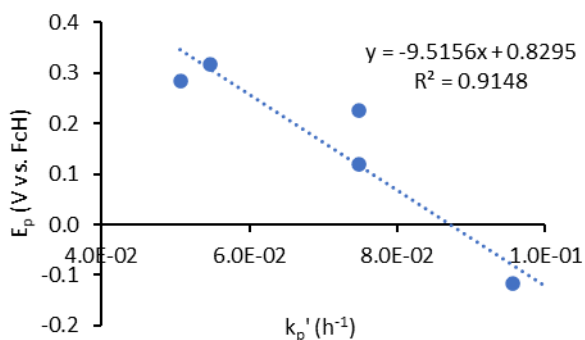


**Fig. 12** Relationship between  $E_{p1}$  and  $k_p'$  for the copper(I) complexes which successfully polymerized MMA.

## Conclusions

Three new copper(I) complexes with iminopyrrolyl ligands were synthesized and characterized by NMR, elemental analysis and, whenever possible, by X-ray diffraction. Starting with 2-iminopyrrolyl

ligand precursors already published by the research group, these complexes were used to study the influence of the steric and electronic environment around the metal center of the complex on the controlled radical polymerization system. To achieve this, the chelating and supporting ligands, were varied. All copper(I) complexes with substituents on position 5 of the pyrrolyl were inactive in polymerization. For the other complexes studied, we observed an influence of the electronic donation effect by the aromatic ring substituents in  $R_2$  in stabilizing the charge on the metal center, as well as a decrease in the polymerization rate for MMA in complexes with higher steric hindrance around the copper. Similarly, an increase in the molecular weight control was observed by decreasing the steric hindrance around the metal center of the complex, yielding values of  $M_n$  closer to the theoretical values. From all the conditions tested, the best result, in terms of controllability of the polymer molecular weight was obtained for complex  $[Cu\{\kappa^2N,N'-NC_4H_3-2-C(H)=NCH_3\}(PMe_3)_2]$  (**10**), by substitution of the phosphine ligand to  $PMe_3$ , which is a better  $\sigma$ -donor than  $PPh_3$ . To complete the analysis of the reactivity of the copper(I) complexes, cyclic voltammetry studies were performed, which allowed for a measurement of the ease of oxidation of each complex. A quasi-linear trend was observed between a lower peak potential for the oxidation of copper(I) to copper(II),  $E_{p1}$ , and the increase in the MMA polymerization rate,  $k_p'$ . The complex with  $PMe_3$  as a support ligand (**10**) was, once again, the one with the lowest value of  $E_{p1}$ , and so, the one most readily oxidized. The PMMA samples obtained presented molecular weight distributions larger than for a pure ATRP mechanism. However, some degree of control for the molecular weight was attained when using the copper(I) complex **10**, being partially in agreement with an ATRP mechanism for the polymerization of MMA.

## Experimental:

**Materials:** All operations involving coordination compounds were performed under nitrogen atmosphere (*Air Liquide*) using suitable glovebox and dual vacuum-nitrogen line techniques. Solvents were dried with molecular sieves and distilled under nitrogen and suitable drying agents (sodium/benzophenone for toluene, diethyl ether and THF; CaH<sub>2</sub> for *n*-hexane and dichloromethane; K<sub>2</sub>CO<sub>3</sub> for DMF). Liquid reagents purification used a general procedure,<sup>14</sup> by drying using a suitable agent (CaH<sub>2</sub> for MMA, MA and styrene; CaCl<sub>2</sub> for acrylonitrile), with stirring under nitrogen atmosphere, followed by *trap-to-trap* distillation. [Cu(NCMe)<sub>4</sub>]BF<sub>4</sub> was synthesized according to the procedure described in the literature.<sup>12</sup>

**General polymerization procedure:** The appropriate mass of metal complex was weighed under nitrogen in a degassed Schlenk tube. The metal complex was dissolved in toluene (or DMF) and the appropriate amount of a solution (in toluene or DMF) of the appropriate radical initiator was added to the previous solution and the temperature set to the desired value. An appropriate amount of monomer was quickly injected into the reaction mixture. Aliquots of the reaction mixture were periodically withdrawn from the reaction mixture. The aliquots content was discharged into a beaker with methanol and the resulting solids filtered and washed with methanol. The solids were dried under vacuum, weighed, and stored in vials. All the samples were analyzed by GPC/SEC and selected samples were analyzed by NMR.

**General procedure for the polymerization of the copper(I) complexes:** 1.2 equiv. of NaH were suspended in THF, in a Schlenk tube. 1.0 equiv. of the respective 2-iminopyrrole ligand precursor was added to the suspension. The mixture was stirred for 30 min, under a slow stream of nitrogen, to

purge the H<sub>2</sub> formed in the reaction. 1.0 equiv. of [Cu(NCMe)<sub>4</sub>]BF<sub>4</sub> was suspended in THF, with 2.0 equiv. of the corresponding phosphine. The solution of the 2-iminopyrrolyl sodium salt was filtered dropwise into the copper starting material suspension, at -20 °C. After the addition, the mixture was allowed to warm to room temperature and was left stirring overnight. The mixture was evaporated to dryness and further extracted with the appropriate solvent, followed by the procedure described for each complex.

**Synthesis of [Cu{κ<sup>2</sup>N,N'-NC<sub>4</sub>H<sub>3</sub>-2-C(H)=N(4-NMe<sub>2</sub>-C<sub>6</sub>H<sub>4</sub>)}(PPh<sub>3</sub>)<sub>2</sub>] (3):** following the general procedure, 0.058 g (2.4 mmol) of NaH, 0.43 g (2.0 mmol) of 2-[N-(4-NMe<sub>2</sub>-C<sub>6</sub>H<sub>4</sub>)formimino]-1*H*-pyrrole, 0.63 g (2.0 mmol) of [Cu(NCMe)<sub>4</sub>]BF<sub>4</sub> and 1.0 g (4.0 mmol) of PPh<sub>3</sub> were used. After the reaction, the solid was extracted with diethyl ether, concentrated until saturation, and stored at -20 °C. A yellow precipitate was filtered out of the solution, dried, and analyzed by <sup>1</sup>H and <sup>31</sup>P NMR, confirming its structure. Yield, 45%.

**Synthesis of [Cu{κ<sup>2</sup>N,N'-NC<sub>4</sub>H<sub>3</sub>-2-C(H)=N(2,6-Me<sub>2</sub>C<sub>6</sub>H<sub>3</sub>)}(PPh<sub>3</sub>)<sub>2</sub>] (7):** following the general procedure, 0.058 g (2.4 mmol) of NaH, 0.40 g (2.0 mmol) of 2-[N-(2,6-Me<sub>2</sub>C<sub>6</sub>H<sub>3</sub>)formimino]-1*H*-pyrrole, 0.63 g (2.0 mmol) of [Cu(NCMe)<sub>4</sub>]BF<sub>4</sub> and 1.0 g (4.0 mmol) of PPh<sub>3</sub> were used. After the reaction, the solid was extracted with toluene and dried under vacuum. Yield, 66%.

Elemental Analysis for C<sub>49</sub>H<sub>43</sub>CuN<sub>2</sub>P<sub>2</sub>, obtained (calculated): C, 74.77 (74.94); H, 5.42 (5.52); N, 3.45 (3.57). <sup>1</sup>H NMR (400 MHz, C<sub>6</sub>D<sub>6</sub>): δ 7.73 (s, 1H, N=CH), 7.37 (m, 1H, H5), 7.28 (m, 12H, PPh<sub>3</sub>-H<sub>ortho</sub>), 7.20 (d, 1H, H4), 7.00-6.85 (m, 21H, PPh<sub>3</sub>-H<sub>meta</sub> + PPh<sub>3</sub>-H<sub>para</sub> + Ar-H<sub>meta</sub> + Ar-H<sub>para</sub> + H5), 6.81 (d, 1H, H3), 1.79 (s, 6H, CH<sub>3</sub>). <sup>13</sup>C{<sup>1</sup>H} NMR (100 MHz, C<sub>6</sub>D<sub>6</sub>): δ 159.3 (N=CH), 151.8 (Ar-C<sub>ipso</sub>), 139.3 (C5), 136.5 (C2), 134.7 (d, PPh<sub>3</sub>-C<sub>ipso</sub>, <sup>1</sup>J<sub>CP</sub> =



22 Hz), 134.0 (d, PPh<sub>3</sub>-C<sub>ortho</sub>, <sup>2</sup>J<sub>CP</sub> = 16 Hz), 130.6 (Ar-C<sub>ortho</sub>), 129.1 (PPh<sub>3</sub>-C<sub>para</sub>), 128.3 (d, PPh<sub>3</sub>-C<sub>meta</sub>, <sup>3</sup>J<sub>CP</sub> = 9.0 Hz), 128.1 (Ar-C<sub>meta</sub>), 123.3 (Ar-C<sub>para</sub>), δ 117.9 (C4), 112.5 (C3), 18.7 (CH<sub>3</sub>). <sup>31</sup>P{<sup>1</sup>H} NMR (121 MHz, C<sub>6</sub>D<sub>6</sub>): δ -1.1 (PPh<sub>3</sub>).

**Synthesis of [Cu{κ<sup>2</sup>N,N'-NC<sub>4</sub>H<sub>3</sub>-2-C(H)=NCH<sub>3</sub>} (PPh<sub>3</sub>)<sub>2</sub>] (8):** following the general procedure, 0.058 g (2.4 mmol) of NaH, 0.22 g (2.0 mmol) of 2-[N-(CH<sub>3</sub>)formimino]-1H-pyrrole, 0.63 g (2.0 mmol) of [Cu(NCMe)<sub>4</sub>]BF<sub>4</sub> and 1.0 g (4.0 mmol) of PPh<sub>3</sub> were used. After the reaction, the solid was extracted with diethyl ether and dried under vacuum, yielding a light pink solid. Crystals were obtained by storing a saturated solution in diethyl ether at 4 °C. Yield, 66%.

Elemental Analysis for C<sub>42</sub>H<sub>37</sub>CuN<sub>2</sub>P<sub>2</sub>, obtained (calculated): C, 72.55 (72.56); H, 5.18 (5.36); N, 4.11 (4.03). <sup>1</sup>H NMR (300 MHz, C<sub>6</sub>D<sub>6</sub>): δ 7.83 (s, 1H, N=CH), 7.54 (br, 1H, H5), 7.38 (m, 12H, PPh<sub>3</sub>-H<sub>ortho</sub>), 6.96 (m, 12H, PPh<sub>3</sub>-H<sub>meta</sub> + PPh<sub>3</sub>-H<sub>para</sub>), 7.05-6.87 (m, 2H, H3 + H4), 2.94 (s, 3H, N-CH<sub>3</sub>). {<sup>1</sup>H} NMR (75 MHz, C<sub>6</sub>D<sub>6</sub>): δ 159.1 (N=CH), 139.3 (C2), 135.4 (C5), 135.1 (PPh<sub>3</sub>-C<sub>ipso</sub>), 133.8 (d, PPh<sub>3</sub>-C<sub>ortho</sub>, <sup>2</sup>J<sub>CP</sub> = 15 Hz), 129.0 (PPh<sub>3</sub>-C<sub>para</sub>), 128.2 (d, PPh<sub>3</sub>-C<sub>meta</sub>, <sup>3</sup>J<sub>CP</sub> = 9.0 Hz), 114.7 (C3), 111.4 (C4), 45.8 (N-CH<sub>3</sub>). <sup>31</sup>P{<sup>1</sup>H} NMR (121 MHz, C<sub>6</sub>D<sub>6</sub>): δ -1.3 (PPh<sub>3</sub>).

**Synthesis of [Cu{κ<sup>2</sup>N,N'-NC<sub>4</sub>H<sub>3</sub>-2-C(H)=NCH<sub>3</sub>} (PMe<sub>3</sub>)<sub>2</sub>] (10):** following the general procedure, 0.026 g (1.2 mmol) of NaH, 0.097 g (0.90 mmol) of 2-[N-(CH<sub>3</sub>)formimino]-1H-pyrrole, 0.28 g (0.90 mmol) of [Cu(NCMe)<sub>4</sub>]BF<sub>4</sub> and 2.0 mL of a 1M solution of PMe<sub>3</sub> in toluene (2.0 mmol) were used. After the reaction, the solid was extracted with *n*-hexane, concentrated until saturation, and stored at -20 °C. After several days pale yellow crystals had formed. Yield, 73%.

Elemental Analysis for C<sub>12</sub>H<sub>25</sub>CuN<sub>2</sub>P<sub>2</sub>, obtained (calculated): C, 40.34 (44.65); H, 6.70 (7.81); N,

8.28 (8.68). Elemental Analysis for C<sub>12</sub>H<sub>14</sub>CuN<sub>4</sub>·Cu·4C<sub>3</sub>H<sub>9</sub>OP, a possible composition after oxidation, obtained (calculated): C, 40.34 (40.62); H, 6.70 (7.10); N, 8.28 (7.89). <sup>1</sup>H NMR (300 MHz, C<sub>6</sub>D<sub>6</sub>): δ 7.80 (s, 1H, N=CH), 7.51 (br, 1H, H5), 7.06 (d, 1H, H3), 6.85 (t, 1H, H4), 3.19 (s, 3H, N-CH<sub>3</sub>), 0.77 (s, 18H, P(CH<sub>3</sub>)<sub>3</sub>). <sup>13</sup>C{<sup>1</sup>H} NMR (75 MHz, C<sub>6</sub>D<sub>6</sub>): δ 159.0 (N=CH), 139.0 (C2), 134.8 (C5), 114.5 (C3), 110.5 (C4), 46.5 (N-CH<sub>3</sub>), δ 15.7 (P(CH<sub>3</sub>)<sub>3</sub>). <sup>31</sup>P{<sup>1</sup>H} NMR (121 MHz, C<sub>6</sub>D<sub>6</sub>): δ -49 (P(CH<sub>3</sub>)<sub>3</sub>).

**Characterizations:** NMR spectra were acquired in a Bruker "AVANCE III" spectrometer, at 300 or 400 MHz. Solution samples were prepared in deuterated solvents (Aldrich), stored at 4 °C (CDCl<sub>3</sub>) or under nitrogen atmosphere (C<sub>6</sub>D<sub>6</sub>, CDCl<sub>3</sub>, 1,1,2,2-tetrachloroethane-*d*<sub>2</sub>, toluene-*d*<sub>8</sub>), at room temperature. Chemical shifts for <sup>1</sup>H and <sup>13</sup>C nuclei were referenced to the residual protio-resonances of the corresponding solvents, which were in turn referenced to tetramethylsilane.

GPC/SEC was performed by eluting HPLC grade THF solutions of the polymeric samples at 30 °C (Waters oven) in two 300×7.5 mm PolyPore columns (protected by a 50×7.5 mm PolyPore guard column) (Polymer Labs) mounted on a Waters 515 isocratic HPLC pump. Detection was performed by a Waters 2414 differential refractive index detector. THF was filtered through 0.45 μm PTFE Pall membrane filters and degassed in an ultrasound bath. Solution samples were filtered through 0.20 μm PTFE Laborspirit filters. The system was calibrated with TSK Tosoh Co. polystyrene standards.

Elemental analyses were conducted at the Laboratório de Análises do Instituto Superior Técnico.

Cyclic voltammetry was performed by using a 10 mg sample of each copper(I) complex, 5 mL of a 0.2 M solution of [N(*n*-Bu)<sub>4</sub>]BF<sub>4</sub> as an auxiliary electrolyte in dry and distilled dichloromethane. The

measurements were performed using a Radiometer DEA 101 Digital Electrochemical Analyzer, coupled to a IMT 102 electrochemical interface. A three-compartment electrochemical cell was used, under nitrogen atmosphere and at ambient temperature, composed of a Pt disc working electrode, a Pt wire auxiliary electrode and a Ag wire reference pseudo-electrode, connected via a Luggin capillary. Scanning speeds of 200 mV s<sup>-1</sup>, 20 mV s<sup>-1</sup> e 2000 mV s<sup>-1</sup> were used. Ferrocene was used as an internal standard to calculate the redox potentials.

Crystallographic data were collected using graphite monochromated Mo-K $\alpha$  radiation ( $\lambda = 0.71073 \text{ \AA}$ ) on a Bruker D8 QUEST diffractometer equipped with an Oxford Cryosystem open-flow nitrogen cryostat, at 150 K. The crystals were selected in air, covered with polyfluoroether oil (*Aldrich*), and mounted on a nylon loop. Cell parameters were retrieved using Bruker SMART<sup>15</sup> software and refined using Bruker SAINT<sup>16</sup> on all observed reflections. Absorption corrections were applied using SADABS.<sup>17</sup> Structure solution and refinement were performed using direct methods with the programs SIR2004<sup>18</sup> and SHELXL-2018/1<sup>19</sup> included in the package of programs WINGX-Version 2014.1.<sup>20</sup> All hydrogen atoms were inserted in idealized positions and allowed to refine riding on the parent carbon atom. All the structures refined to a perfect convergence. Graphic presentations were prepared with Mercury 2020.3.0.<sup>21</sup>

## References

- (1) Szwarc, M. *Nature* **1956**, *178*, 1168–1169.
- (2) Matyjaszewski, K. *ACS Symp. Ser.* **2000**, *768*, 2–26.
- (3) Boyer, C.; Corrigan, N. A.; Jung, K.; Nguyen, D.; Nguyen, T. K.; Adnan, N. N. M.; Oliver, S.; Shanmugam, S.; Yeow, J. *Chem. Rev.* **2016**, *116*, 1803–1949.
- (4) Jakubowski, W.; Min, K.; Matyjaszewski, K. *Macromolecules* **2006**, *39*, 39–45.
- (5) Chmielarz, P. et al. *Progress in Polymer Science*. Pergamon June 1, 2017, pp 47–78.
- (6) Lorandi, F. et al. *Current Opinion in Electrochemistry*. Elsevier March 1, 2018, pp 1–7.
- (7) Rodrigues, A. I.; Figueira, C. A.; Gomes, C. S. B.; Suresh, D.; Ferreira, B.; Di Paolo, R. E.; De Sa Pereira, D.; Dias, F. B.; Calhorda, M. J.; Morgado, J.; Maçanita, A. L.; Gomes, P. T. *Dalton Trans.* **2019**, *48*, 13337–13352.
- (8) Suresh, D.; Lopes, P. S.; Ferreira, B.; Figueira, C. A.; Gomes, C. S. B.; Gomes, P. T.; Di Paolo, R. E.; Maçanita, A. L.; Duarte, M. T.; Charas, A.; Morgado, J.; Calhorda, M. J. *Chem. - Eur. J.* **2014**, *20*, 4126–4140.
- (9) Carabineiro, S. A.; Bellabarba, R. M.; Gomes, P. T.; Pascu, S. I.; Veiros, L. F.; Freire, C.; Pereira, L. C. J.; Henriques, R. T.; Conceição Oliveira, M.; Warren, J. E. *Inorg. Chem.* **2008**, *47*, 8896–8911.
- (10) Krishnamoorthy, P.; Ferreira, B.; Gomes, C. S. B.; Vila-Viçosa, D.; Charas, A.; Morgado, J.; Calhorda, M. J.; Maçanita, A. L.; Gomes, P. T. *Dyes Pigm.* **2017**, *140*, 520–532.
- (11) Carabineiro, S. A.; Silva, L. C.; Gomes, P. T.; Pereira, L. C. J.; Veiros, L. F.; Pascu, S. I.; Duarte, M. T.; Namorado, S.; Henriques, R. T. *Inorg. Chem.* **2007**, *46*, 6880–6890.
- (12) Kubas, G. J.; Monzyk, B.; Crumblis, A. L. *Inorganic Syntheses: Reagents for Transition Metal Complex and Organometallic Syntheses, vol. 28*; John Wiley & Sons, Ltd, 1990; pp 68–70.
- (13) Müller, T. E.; Mingos, D. M. P. *Transit. Met. Chem.* **1995**, *20*, 533–539.
- (14) Armarego, W. L. F.; Perrin, D. D. *Purification of Laboratory Chemicals*, 4<sup>a</sup> ed.; Butterworth Heinemann, 1997.
- (15) SMART Software for the CCD Detector System Version 5.625, Bruker AXS Inc., Madison, WI, USA, 2001.
- (16) SAINT Software for the CCD Detector System, Version 7.03, Bruker AXS Inc., Madison, WI, USA, 2004.
- (17) Sheldrick, G. M. SADABS, Program for Empirical Absorption Correction, University of Gottingen, Go'ttingen, 1996.
- (18) Burla, M. C.; Caliandro, R.; Camalli, M.; Carrozzini, B.; Cascarano, G. L.; De Caro, L.; Giacovazzo, C.; Polidori, G.; Spagna, R. *J. Appl. Crystallogr.* **2005**, *38*, 381–388.
- (19) (a) Sheldrick, M. *Acta Crystallogr., Sect. C: Struct. Chem.* **2015**, *71*, 3–8. (b) Hübschle, C. B.; Sheldrick, G. M.; Dittrich, B. *J. Appl. Crystallogr.* **2011**, *44*, 1281–1284.
- (20) Farrugia, L. J. *J. Appl. Crystallogr.* **1999**, *32*, 837–838.
- (21) Macrae, C. F.; Edgington, P. R.; McCabe, P.; Pidcock, E.; Shields, G. P.; Taylor, R.; Towler, M.; van de Streek, J. *J. Appl. Crystallogr.* **2006**, *39*, 453–457.